Broadband Dipole Absorption in Dispersive Photonic Time Crystals

Thomas F. Allard,* Jaime E. Sustaeta-Osuna, Francisco J. García-Vidal, and Paloma A. Huidobro
Departamento de Física Teórica de la Materia Condensada, Universidad Autónoma de Madrid, E-28049 Madrid, Spain
and Condensed Matter Physics Center (IFIMAC), Universidad Autónoma de Madrid, E-28049 Madrid, Spain

(Received 7 August 2025; revised 19 November 2025; accepted 2 February 2026; published 11 March 2026)

Photonic media modulated periodically in time, termed photonic time crystals (PTCs), have attracted considerable attention for their ability to open momentum bandgaps hosting amplifying modes. These momentum gaps, however, generally appear only at the system's parametric resonance condition which constrain many features derived from amplification to a narrow frequency band. Moreover, they are accompanied by exceptional points (EPs) and may drive the system into an instability, which renders their analysis more intricate. Here, we show that a careful consideration of dispersion and absorption can overcome these issues. By investigating the dissipated power of a point-dipole embedded in a dispersive and absorptive PTC, we unveil that temporal modulation enables the conversion of dipole emission into dipole absorption within a broadband frequency window free of EPs. We demonstrate that this effect is general, emerging in both the stable and unstable regimes, and occurs from weak modulation strength to low modulations frequencies that could be achieved for various material platforms.

DOI: 10.1103/gttv-6lqc

Introduction—A sudden change in a material refractive index—a time interface—induces frequency conversion accompanied by both forward and backward propagating waves, a phenomenon termed time refraction and reflection [1,2]. While early studies predicted these effects decades ago [3,4], recent experimental advances have led to a surge in interest in the photonics of time-varying media, aiming at new possibilities of wave manipulation [5–9]. Unique phenomena without counterpart in static systems have since been proposed [10–20] and time reflection has been observed in transmission line metamaterials [21,22]. Moreover, ultrafast modulation of the refractive index in transparent conductive oxides (TCOs) [23,24] paves the way for time-varying media in the optical regime [25–28].

Within this burgeoning field, materials whose electric permittivity is modulated periodically in time [29]—termed photonic time crystals (PTCs)—have attracted much attention [30]. Indeed, periodic modulation induces interference between time-refracted and -reflected waves, which open momentum bandgaps that host amplifying and decaying modes, allowing energy transfer between the temporal modulation and electromagnetic waves propagating through the material.

*Contact author: thomas.allard@uam.es

Published by the American Physical Society under the terms of the Creative Commons Attribution 4.0 International license. Further distribution of this work must maintain attribution to the author(s) and the published article's title, journal citation, and DOI.

Although many effects can be drawn from simplified models of PTCs, the inclusion of realistic aspects such as material dispersion and losses becomes essential to accurately model experiments [30–35]. Frequency dispersion also complexifies the concept of momentum gap, as it can induce extended gaps [36], as well as dispersive ones [37–39], namely, broadband *frequency* windows of potentially amplifying modes. The latter stand in sharp contrast with momentum gaps of nondispersive PTCs that, while encompassing many momenta, are constrained to the parametric resonance (PR) condition, i.e., to half of the modulation frequency.

A key question in the field of PTCs is their interaction with emitters. Notably, what is their impact on dipole radiation and its quantum counterpart, spontaneous emission? Enhanced charge radiations in PTCs have been predicted [40,41], and the authors of Ref. [42] reported amplified emission from a dipolar emitter embedded in a nondispersive, lossless PTC, along with a modification of the spontaneous emission decay near the momentum gap frequency, depending on the initial modulation profile [43]. On the other hand, the authors of Ref. [44] recently proposed a classical non-Hermitian formalism considering losses. They demonstrated that the spontaneous emission modification, proportional to the dipole's dissipated power, is accompanied by spontaneous excitation, which manifests classically as a negative dissipated power. This negative power is intrinsic to the gain available in PTCs and can be interpreted as dipole *absorption*.

Importantly, the above theoretical studies revealed three *a priori* major drawbacks of PTCs. First, the emission

modification is constrained around the PR condition, making it very narrow band, a phenomenon recently observed experimentally using transmission-line metamaterials [45]. Second, this particular frequency is associated to divergencies [43,44], and overlaps with exceptional points (EPs) [46,47]. These non-Hermitian degeneracies, while offering potential interest for sensing [48], increase the spontaneous emission rate independently of amplification [49], which obscures the effect of the temporal modulation itself. Third, amplifying modes of momentum gaps drive the system into an instability, greatly complicating the analysis.

In this Letter, we overcome these limitations by carefully considering dispersion and losses in our theoretical framework. By investigating the dissipated power of a dipole embedded in a dispersive and absorptive PTC, we unveil new regimes of modulation where dispersive momentum gaps as well as negative Floquet replicas allow the conversion of emission into absorption in broadband frequency ranges. Additionally, we show that inevitable losses eliminate EPs from dispersive momentum gaps, allowing us to disentangle the impacts of these points from those of modulation-induced gain. We demonstrate that these effects are general, occurring from small modulation strengths to low modulation frequencies, for different material platforms, and in both the stable and unstable regimes of a PTC.

Dispersive and absorptive PTC—The system under consideration, sketched in Fig. 1(a), is modeled by the combination of Maxwell's equations $\nabla \times \mathbf{E} = -\mu_0 \partial_t \mathbf{H}$ and $\nabla \times \mathbf{H} = \partial_t \mathbf{D} + \mathbf{J}$ with the parametric Drude-Lorentz model

$$\partial_t^2 \mathbf{P} + \gamma \partial_t \mathbf{P} + \omega_0^2 \mathbf{P} = \epsilon_0 \omega_p^2 \mathbf{E} \tag{1}$$

that describes the dynamics of the three-dimensional polarization density $\mathbf{P}$ inside a general dispersive medium. Here, γ, ω_p and ω_0 are the material's inverse relaxation time, plasma, and resonance frequency.

Importantly, our Letter aims at capturing the essential physics of various time-modulated platforms. To this end, we consider a periodic modulation in time of either the plasma or the resonance frequency as $\omega_{p/0}^2(t) = \omega_{p/0}^2[1 + \alpha \sin(\Omega t)]$, with Ω and α the modulation's frequency and strength, respectively. A time-dependent plasma frequency typically models ultrafast optical pumping of TCOs in the epsilon-near-zero (ENZ) regime [23], where order-unity refractive index changes have been realized in both thin films [14,26] and ENZ-based resonant metasurfaces [25,50]. Recent promising experiments also demonstrated order-unity and subcycle periodic modulation of the conduction band electrons effective mass in a surface plasmon cavity metamaterial operating at terahertz frequencies [51]. On the other hand, a time-dependent resonant frequency can be emulated by spatially structuring a modulated medium [36], by modulating the optical phonon frequency of polar insulators [52,53], or by varying the capacitance in state-of-the-art transmission-line metamaterials [21,54], for which the interaction between a dipole and a PTC has been recently measured [45].

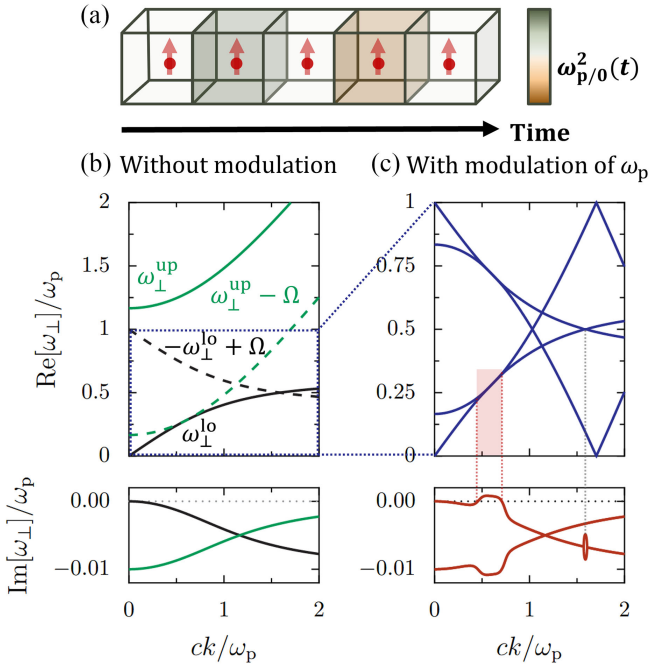


FIG. 1. (a) Sketch of the system under consideration. A three-dimensional Drude-Lorentz medium, with either its plasma or resonance frequency modulated sinusoidally in time, contains an oscillating dipole. (b),(c) Formation of dispersive momentum gaps. (b) Complex bandstructure of the static medium ($\alpha = 0$). Dashed lines represent Floquet replicas of the original bands, shifted by a modulation frequency $\Omega = \omega_p$. (c) Complex bandstructure of a medium with a modulated plasma frequency ($\alpha = 0.05$) in the first FBZ. The red area highlights the modulation-induced gain region. In both panels, $\omega_0 = 0.6\omega_p$ and, as in the remaining of this Letter, $\gamma = 0.02\omega_p$.

To obtain the fields in the medium, we follow Ref. [55] and combine Maxwell's equations with Eq. (1) into a Schrödinger-like matrix problem using the auxiliary field $\dot{\mathbf{P}} = \partial_t \mathbf{P}$. Following Ref. [44], we solve this problem using a Floquet formalism, detailed in Supplemental Material (SM) [56]. It is noteworthy that the complexity of our model accounts for the role of both longitudinal and transverse fields. Recent works have shown that longitudinal modes can also undergo amplification in PTCs [61,62]. Using an hydrodynamic nonlocal model, we demonstrate in SM [56] that longitudinal modes may indeed also modify a dipole's emission in a broadband manner. In the main text we focus however on transverse modes, as they match experiments using transmission-line metamaterials [45,54].

EP-free dispersive momentum gaps—Without modulation, the Drude-Lorentz model features transverse modes with a two-band complex bandstructure. The upper and lower bands, denoted as $\omega_\perp^{up}$ and $\omega_\perp^{lo}$, are represented in Fig. 1(b). The temporal periodicity in the modulation

frequency Ω causes the folding of the bandstructure in the first Floquet Brillouin Zone (FBZ) $\omega \in [0, \Omega]$, inducing positive and negative Floquet replicas $\pm\omega_\perp^{\mathrm{up/lo}} + n\Omega$, with $n \in \mathbb{Z}$. In the modulated system, these replicas may interact with each other, through either an avoided crossing or their merging, which occurs at EPs [46,47]. Such a degeneracy of two replicas is what leads to momentum gaps, regions hosting a pair of eigenfrequencies with, respectively, increased and decreased imaginary parts with respect to the nonmodulated value. Depending on a competition between modulation strength and material losses, these regions can host amplified eigenmodes with $\mathrm{Im}[\omega_\perp] > 0$ [30].

In nondispersive PTCs, these gaps are single-frequency so that we term them in the following as "flat." They arise only at multiples of the PR condition, where an eigenmode ω is degenerate with one of its own negative replicas $-\omega + n\Omega$. The two-band nature of a Drude-Lorentz PTC, however, enables new possibilities, such as the merging of the lower band with a replica of the upper band. From their shape difference, this can lead to a dispersive, broadband in frequency, momentum gap [37–39]. We note that although we here leverage dispersion to achieve this phenomenon, it can also been found through space-time modulations [63] or anisotropy [48,64,65].

The complex bandstructure of a medium with modulated plasma frequency is presented in Fig. 1(c) and illustrates that mechanism. Here, the modulation frequency Ω is chosen so that the lower band $\omega_\perp^{\mathrm{lo}}$ couples with a downshifted replica of the upper band $\omega_\perp^{\mathrm{up}} - \Omega$. By considering a modulation strength α large enough to counteract the material losses γ, this leads to a broadband gain region where the eigenfrequency's imaginary part is positive (see the red area), which drives the PTC into its unstable regime. Importantly, dispersive momentum gaps originating from the coupling between two bands with a different imaginary dispersion, the inclusion of losses induces the imaginary component of the band to split in two within the gap. This, critically, eliminates the EPs associated with dispersive momentum gaps. In contrast, a flat momentum gap which preserves the EPs is still present at $\Omega/2$, but losses prevent it from allowing gain [see Fig. 1(c)]. We discuss the impact of losses on EPs through a calculation of the phase rigidity [66] in SM [56].

Interestingly, these EP-free momentum gaps occur in a wide range of parameters when modulating the plasma frequency. Indeed, a simple analytical calculation shows that the condition $\omega_\perp^{\mathrm{lo}} = \omega_\perp^{\mathrm{up}} - n\Omega$ is satisfied as long as $n\Omega \geq \omega_{\mathrm{p}}$ [56]. While a small modulation strength only enables the first-order replica $n = 1$ to interact, increasing α allows for higher-order replicas to contribute, lowering the required modulation frequency. Notably, when $n\Omega = \omega_{\mathrm{p}}$ the two bands are degenerate at $ck = \omega_0$, allowing a crossing in the dispersive part of $\omega_\perp^{\mathrm{lo}}$, hence maximizing the gain bandwidth.

Broadband dipole absorption—To embed an harmonic dipole oscillating at a frequency ω in the PTC, we set the source current density as $\mathbf{J}(\mathbf{r}, t) = -i\omega\mathbf{p}(t)\delta(\mathbf{r})$, with $\mathbf{p}(t) = |\mathbf{p}|e^{-i\omega t}\hat{p}$ being the dipole moment. The transverse field contribution of the power dissipated by the source is $P_\omega^\perp(t) = (\omega/2)\,\mathrm{Im}[\mathbf{p}^*(t) \cdot \mathbf{E}^\perp(\mathbf{0}, t)]$. Its time and orientation average can be rewritten as

$$\bar{P}_\omega^\perp = \frac{\pi\omega^2|\mathbf{p}|^2}{12\epsilon_0}\int_{\mathbb{R}^3} d^3\mathbf{k}\tilde{\rho}_{k,\omega}^\perp. \tag{2}$$

Here, $\tilde{\rho}_{k,\omega}^\perp$ is the transverse part of the photonic momentum-resolved local density of states (LDOS), a quantity recently measured in a transmission-line-based PTC [45], and which we compute through the Floquet Green dyadic of the fields [56]. As shown in Ref. [44], the gain mechanism induced by the temporal modulation reveals itself through regions of reciprocal space with negative LDOS. To analyze our results, we thus separate the positive and negative contributions of the LDOS to the dissipated power, and define $\bar{P}_\omega^{\perp,\mathrm{loss(gain)}}$ as the integral over reciprocal space where the LDOS is positive (negative) [44,67]. In that way, the total power $\bar{P}_\omega^{\perp,\mathrm{total}} = \bar{P}_\omega^{\perp,\mathrm{loss}} - \bar{P}_\omega^{\perp,\mathrm{gain}}$. Importantly, such a calculation of dissipated power, as done in previous studies [42–44], only reflects the effect of the modulation *on the dipole itself*. It does not account for the fields within the medium growing exponentially over time if the PTC operates in its unstable regime, with eigenfrequencies of positive imaginary part. In that case, the quantity (2) is dominant only during the early-time dynamics of the system, when $t \ll 1/\max(\mathrm{Im}[\omega_\perp])$.

The momentum-resolved LDOS, or spectral function, is presented alongside the real Floquet bandstructure in Fig. 2(a) in the scenario of weak yet fast modulation of the plasma frequency we exemplified in Fig. 1(c). The LDOS is, as expected, positively peaked (blueish) along the original lower band $\omega_\perp^{\mathrm{lo}}$. Remarkably, however, a negative peak (reddish) is also present along the first downshifted replica of the upper band, $\omega_\perp^{\mathrm{up}} - \Omega$. Within the EP-free dispersive momentum gap generated by the coupling between these two bands, the negative spectral function arising from the downshifted replica dominates and supersedes the original positive peak. This mechanism induces, as visible in Fig. 2(c), a large broadband gain contribution to the dissipated power (red line), together with an inhibition of the loss contribution (blue line). Interestingly, both contributions present sharp peaks precisely at the boundaries of the gain bandwidth, where $\mathrm{Im}[\omega_\perp] = 0$ This is similar to what is found for flat momentum gaps, for which a divergence occurs at the EP's frequency [43] precisely due to momenta corresponding to real eigenfrequencies where the LDOS exhibits poles [44]. The absence of EPs in our context confirms that these divergences and the associated peaks

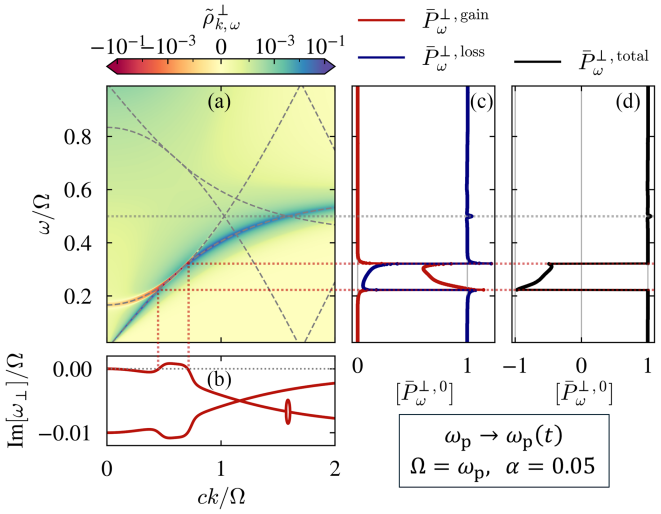


FIG. 2. Broadband dipole absorption through weak modulation of the plasma frequency. (a) Momentum-resolved LDOS. The gray dashed lines show the real Floquet bandstructure $\text{Re}[\omega_\perp]$. (b) Imaginary Floquet bandstructure. (c) Positive $\bar{P}^{\perp,\text{loss}}_{\omega}$ and negative $\bar{P}^{\perp,\text{gain}}_{\omega}$ parts of the power dissipated by a point dipole with frequency ω, in units of the nonmodulated value $\bar{P}^{\perp,0}_{\omega}$. (d) Total dissipated power $\bar{P}^{\perp,\text{total}}_{\omega} = \bar{P}^{\perp,\text{loss}}_{\omega} - \bar{P}^{\perp,\text{gain}}_{\omega}$.

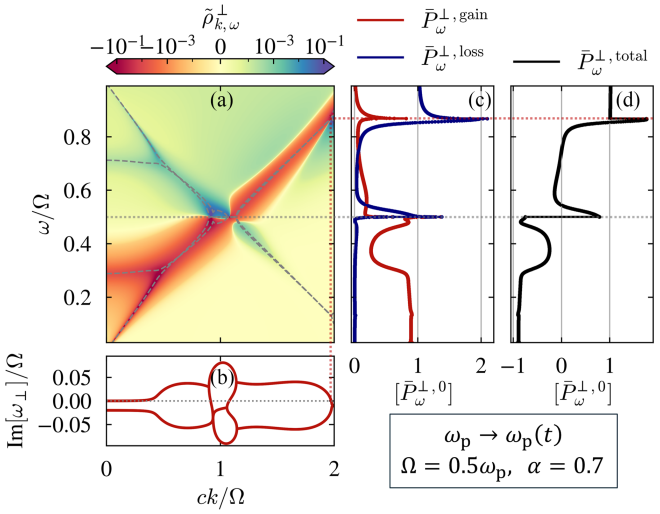


FIG. 3. Broadband absorption and inhibition of dissipated power. Same quantities as in Fig. 2, but considering a stronger yet lower modulation of the plasma frequency.

in dissipated power are not linked to exceptional-point physics [68].

The total dissipated power, shown in Fig. 2(d), hence exhibits negative values up to 1 times what is found without modulation, in a bandwidth of about 0.1Ω. We interpret this negative dissipated power as the absorption—instead of emission—of energy by the dipole, the temporal modulation transferring energy to the source, converting it into a sink. Regarding the late-time dynamics, the broadband in frequency nature of the momentum gap let us predict a spectrally broad amplification of noise by the unstable PTC, in contrast with the narrow-band lasing induced by flat momentum gaps [45]. Away from the dispersive momentum gap, the dissipated power is unchanged from that of a nonmodulated system, except for a slight increase at $\omega = \Omega/2$. Indeed, the flat momentum gap, although not allowing any gain, induces an enhancement of dipole emission solely due to the EPs at its edges [49].

We now turn our attention to a scenario of plasma frequency modulation strong enough to allow several Floquet replicas to interact with each other, adding complexity to both the band structure and LDOS. For the second-order replica $\omega^{\text{up}}_\perp - 2\Omega$ to play the same role as the first-order one in the previous case, we consider a modulation with frequency $\Omega = \omega_\text{p}/2$ and strength $\alpha = 0.7$. The same quantities as discussed previously are shown for that case in Fig. 3. Here, the interaction between $\omega^{\text{up}}_\perp - 2\Omega$ and $\omega^{\text{lo}}_\perp$ induces a dispersive momentum gap occupying the majority of the first FBZ. Modulating at $\Omega = \omega_\text{p}/2$ also induces a flat momentum gap between $\omega^{\text{lo}}_\perp$ and $-\omega^{\text{lo}}_\perp + \Omega$ in the same region as the dispersive one, leading to an interplay that results in a larger value of positive imaginary part for the concerned eigenmodes [see Fig. 3(b)].

As visible in Fig. 3(a), the downshifted replica is again associated to negative peaks of the LDOS and converts the radiation of the lower band $\omega^{\text{lo}}_\perp$ into absorption in a wide bandwidth, suppressing the emission contribution of the dissipated power $\bar{P}^{\perp,\text{loss}}_{\omega}$[see Fig. 3(c)]. Interestingly, the splitting of the imaginary bands in two induced by losses allows for slightly positive imaginary parts at small momenta, further broadening the gain bandwidth. The negative LDOS is however narrower and smaller at large wave numbers, leading to a peculiar structure which reflects in the total dissipated power as two regimes of dipole frequencies [see Fig. 3(d)]. Below the PR condition ($\omega < \Omega/2$), the modulation-induced gain dominates and the dipole's emission is converted into absorption, with an almost unit ratio for small frequencies. Above it ($\omega > \Omega/2$), however, both positive and negative LDOS values are small as compared to the nonmodulated case, resulting in a broadband suppression of dissipated power. In that sense, the modulation-induced gain counteracts the dipole's regular emission and generates an effective frequency band gap for the dipole, in which dissipated power is inhibited. Two sharp peaks at $\omega = \Omega/2$ and $\omega \simeq 0.87\Omega$ are also visible in the dissipated power, originating from poles of the LDOS where $\text{Im}[\omega_\perp] = 0$ [see Fig. 3(b) near $ck \simeq \Omega$ and $ck \simeq 2\Omega$]. At $\Omega/2$, a pair of EPs is also present, complicating the interpretation. Finally, we stress that while we focused here on an unstable PTC, a modulated plasma frequency also allows significant modifications of a dipole's emission without relying on eigenmodes with positive imaginary part, as exemplified in SM [56].

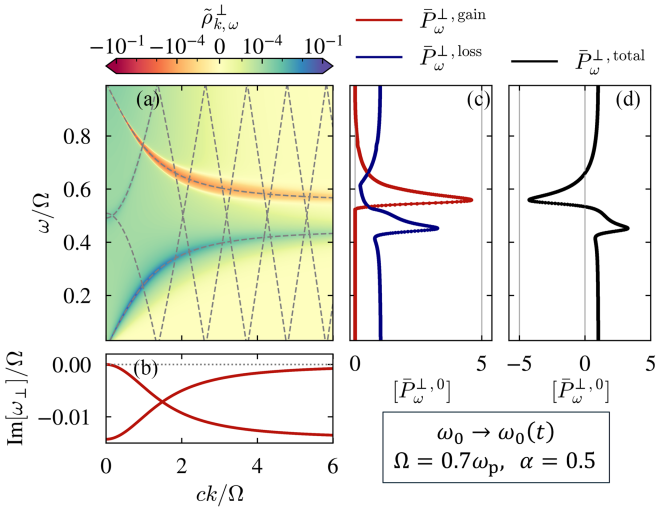


FIG. 4. Drastic enhancement of emission and absorption in a stable PTC. Same quantities as in Figs. 2 and 3, but considering a modulation of the resonance frequency around the value $\omega_0 = 0.3\omega_{\mathrm{p}}$.

Modulated resonance frequency—As discussed in the presentation of our model, PTCs have been realized experimentally using different forms of temporal modulation. This motivates us to also examine a medium whose resonance frequency is modulated in time, for which we present the momentum-resolved LDOS and complex band structure in Figs. 4(a) and 4(b).

Considering a resonance frequency $\omega_0 = 0.3\omega_{\mathrm{p}}$ modulated with strength $\alpha = 0.5$ and frequency $\Omega = 0.7\omega_{\mathrm{p}} > 2\omega_0$, we place ourselves in a regime where the lower band and its own negative replica do not interact (see SM for detail [56]). In this way, no momentum gap is present, thereby keeping the PTC stable. Hence, the dissipated power (2) accurately represents the steady-state quantity, as no exponentially growing transient is present. Critically, however, two distinct processes still allow a drastic and broadband modification of the dissipated power in that scenario. First, the lower band, associated to positive LDOS, is slightly blue shifted as compared to the nonmodulated case. This induces a large LDOS in an almost flat band where it is nearly zero without modulation, producing an increase of the loss contribution to dissipated power up to 3 times the static value [see Fig. 4(c)]. Second, and in stark contrast with the plasma frequency modulation, here replicas of negative frequencies, such as $-\omega^{\mathrm{lo}}_{\perp} + \Omega$, are associated to negative LDOS. This enables the input of gain within all the frequency bandgap between the original lower and upper bands, and especially around its asymptotic close to $-\omega_0 + \Omega$. Interestingly, such a gain mechanism driven by negative replicas without momentum gaps also emerges in a plasmonic time crystal slab [69]. Together, these processes leverage dispersion to enable either the enhancement of total emission, or the broadband absorption of a dipole, depending on its frequency being below or above the PR condition [see Fig. 4(d)]. As this phenomenon does not occur when modulating the plasma frequency, it makes the modulation of a material's resonance a promising way of modifying dipole emission.

Conclusions—In this Letter, we provided a comprehensive study of the power dissipated by a point dipole embedded in a photonic time crystal. We leveraged dispersion and absorption to unveil that temporal modulation enables a broadband in frequency conversion of dipole emission into dipole absorption that occurs across a wide range of modulation parameters and in both cases of modulated plasma and resonance frequencies. In addition, for modulated resonance frequency, we demonstrated the possibility of both a broadband negative dissipated power and a large enhancement of emission while operating in the PTC's stable regime. In our considered scenarios, these phenomena appear independently of exceptional points, allowing us to disentangle the effects associated to the latter from those of gain. From the classical-quantum correspondence between dipole radiation and spontaneous emission [70], our Letter, although being classical, paves the way for the investigation of quantum effects in PTCs [71–75]. In particular, our results suggest that temporal modulation may force a multi-level emitter either to remain in its excited state or to climb its energy ladder through spontaneous excitation [44,75], depending on its frequency, opening exciting perspectives in the field of time-varying media.

Acknowledgments—We acknowledge funding from the European Union through the ERC grant TIMELIGHT under No. GA 101115792, and from the Spanish Ministry for Science, Innovation, and Universities—Agencia Estatal de Investigación (AEI) through Grants No. PID2022-141036NA-I00, No. PID2024-161142NB-I00, and No. CEX2018-000805-M (through the María de Maeztu program for Units of Excellence in Research and Developments) and Grant No. RYC2021-031568-I (Ramón y Cajal program). J. E. S.-O. also acknowledges support from the CAM Consejería de Educación, Ciencia y Universidades, Viceconsejería de Universidades, Investigación y Ciencia, Dirección General de Investigación e Innovación Tecnológica (CAM FPI Grant Ref. A281).

Data availability—The data that support the findings of this article are openly available [76].

[1] J. T. Mendonça and P. K. Shukla, Time refraction and time reflection: Two basic concepts, Phys. Scr. **65**, 160 (2002).
[2] V. Bacot, M. Labousse, A. Eddi, M. Fink, and E. Fort, Time reversal and holography with spacetime transformations, Nat. Phys. **12**, 972 (2016).

[3] F. Morgenthaler, Velocity modulation of electromagnetic waves, IEEE Trans. Microw. Theory Tech. **6**, 167 (1958).
[4] L. Felsen and G. Whitman, Wave propagation in time-varying media, IEEE Trans. Antennas Propag. **18**, 242 (1970).
[5] M. Z. Alam, I. D. Leon, and R. W. Boyd, Large optical nonlinearity of indium tin oxide in its epsilon-near-zero region, Science **352**, 795 (2016).
[6] A. M. Shaltout, V. M. Shalaev, and M. L. Brongersma, Spatiotemporal light control with active metasurfaces, Science **364**, eaat3100 (2019).
[7] J. Bohn, T. S. Luk, C. Tollerton, S. W. Hutchings, I. Brener, S. Horsley, W. L. Barnes, and E. Hendry, All-optical switching of an epsilon-near-zero plasmon resonance in indium tin oxide, Nat. Commun. **12**, 1017 (2021).
[8] E. Galiffi, R. Tirole, S. Yin, H. Li, S. Vezzoli, P. A. Huidobro, M. G. Silveirinha, R. Sapienza, A. Alù, and J. B. Pendry, Photonics of time-varying media, Adv. Opt. Photonics **4**, 014002 (2022).
[9] S. Yin, E. Galiffi, and A. Alù, Floquet metamaterials, eLight **2**, 8 (2022).
[10] Z. Yu and S. Fan, Complete optical isolation created by indirect interband photonic transitions, Nat. Photonics **3**, 91 (2009).
[11] D. L. Sounas and A. Alù, Non-reciprocal photonics based on time modulation, Nat. Photonics **11**, 774 (2017).
[12] Z.-L. Deck-Léger, N. Chamanara, M. Skorobogatiy, M. G. Silveirinha, and C. Caloz, Uniform-velocity spacetime crystals, Adv. Opt. Photonics **1**, 056002 (2019).
[13] V. Pacheco-Peña and N. Engheta, Antireflection temporal coatings, Optica **7**, 323 (2020).
[14] Y. Zhou, M. Z. Alam, M. Karimi, J. Upham, O. Reshef, C. Liu, A. E. Willner, and R. W. Boyd, Broadband frequency translation through time refraction in an epsilon-near-zero material, Nat. Commun. **11**, 2180 (2020).
[15] H. Li, S. Yin, E. Galiffi, and A. Alù, Temporal parity-time symmetry for extreme energy transformations, Phys. Rev. Lett. **127**, 153903 (2021).
[16] V. Pacheco-Peña and N. Engheta, Temporal equivalent of the Brewster angle, Phys. Rev. B **104**, 214308 (2021).
[17] F. R. Prudêncio and M. G. Silveirinha, Synthetic axion response with space-time crystals, Phys. Rev. Appl. **19**, 024031 (2023).
[18] J. E. Vázquez-Lozano and I. Liberal, Incandescent temporal metamaterials, Nat. Commun. **14**, 4606 (2023).
[19] Z. Hayran and F. Monticone, Beyond the Rozanov bound on electromagnetic absorption via periodic temporal modulations, Phys. Rev. Appl. **21**, 044007 (2024).
[20] K. S. Eswaran, A. E. Kopaei, and K. Sacha, Anderson localization in photonic time crystals, Phys. Rev. B **111**, L180201 (2025).
[21] H. Moussa, G. Xu, S. Yin, E. Galiffi, Y. Ra'di, and A. Alù, Observation of temporal reflection and broadband frequency translation at photonic time interfaces, Nat. Phys. **19**, 863 (2023).
[22] X. Wang, M. S. Mirmoosa, V. S. Asadchy, C. Rockstuhl, S. Fan, and S. A. Tretyakov, Metasurface-based realization of photonic time crystals, Sci. Adv. **9**, eadg7541 (2023).
[23] O. Reshef, I. De Leon, M. Z. Alam, and R. W. Boyd, Nonlinear optical effects in epsilon-near-zero media, Nat. Rev. Mater. **4**, 535 (2019).
[24] I.-W. Un, S. Sarkar, and Y. Sivan, Electronic-based model of the optical nonlinearity of low-electron-density Drude materials, Phys. Rev. Appl. **19**, 044043 (2023).
[25] S. Vezzoli, V. Bruno, C. DeVault, T. Roger, V. M. Shalaev, A. Boltasseva, M. Ferrera, M. Clerici, A. Dubietis, and D. Faccio, Optical time reversal from time-dependent epsilon-near-zero media, Phys. Rev. Lett. **120**, 043902 (2018).
[26] R. Tirole, S. Vezzoli, E. Galiffi, I. Robertson, D. Maurice, B. Tilmann, S. A. Maier, J. B. Pendry, and R. Sapienza, Double-slit time diffraction at optical frequencies, Nat. Phys. **19**, 999 (2023).
[27] E. Lustig, O. Segal, S. Saha, E. Bordo, S. N. Chowdhury, Y. Sharabi, A. Fleischer, A. Boltasseva, O. Cohen, V. M. Shalaev, and M. Segev, Time-refraction optics with single cycle modulation, Nanophotonics **12**, 2221 (2023).
[28] R. Tirole, S. Vezzoli, D. Saxena, S. Yang, T. V. Raziman, E. Galiffi, S. A. Maier, J. B. Pendry, and R. Sapienza, Second harmonic generation at a time-varying interface, Nat. Commun. **15**, 7752 (2024).
[29] J. R. Zurita-Sánchez, P. Halevi, and J. C. Cervantes-González, Reflection and transmission of a wave incident on a slab with a time-periodic dielectric function $\epsilon(t)$, Phys. Rev. A **79**, 053821 (2009).
[30] M. M. Asgari, P. Garg, X. Wang, M. S. Mirmoosa, C. Rockstuhl, and V. Asadchy, Theory and applications of photonic time crystals: A tutorial, Adv. Opt. Photonics **16**, 958 (2024).
[31] D. M. Solís and N. Engheta, Functional analysis of the polarization response in linear time-varying media: A generalization of the Kramers-Kronig relations, Phys. Rev. B **103**, 144303 (2021).
[32] M. S. Mirmoosa, T. Koutserimpas, G. Ptitcyn, S. Tretyakov, and R. Fleury, Dipole polarizability of time-varying particles, New J. Phys. **24**, 063004 (2022).
[33] S. A. R. Horsley, E. Galiffi, and Y.-T. Wang, Eigenpulses of dispersive time-varying media, Phys. Rev. Lett. **130**, 203803 (2023).
[34] J. Sloan, N. Rivera, J. D. Joannopoulos, and M. Soljacic, Optical properties of dispersive time-dependent materials, ACS Photonics **11**, 950 (2024).
[35] T. T. Koutserimpas and F. Monticone, Time-varying media, dispersion, and the principle of causality [Invited], Opt. Mater. Express **14**, 1222 (2024).
[36] X. Wang, P. Garg, M. S. Mirmoosa, A. G. Lamprianidis, C. Rockstuhl, and V. S. Asadchy, Expanding momentum bandgaps in photonic time crystals through resonances, Nat. Photonics **19**, 149 (2025).
[37] F. Feng, N. Wang, and G. P. Wang, Temporal transfer matrix method for lorentzian dispersive time-varying media, Appl. Phys. Lett. **124**, 101701 (2024).
[38] M. G. Ozlu, V. Mkhitaryan, C. B. Fruhling, A. Boltasseva, and V. M. Shalaev, Floquet engineering of polaritonic amplification in dispersive photonic time crystals, Phys. Rev. Res. **7**, 023214 (2025).
[39] Y.-T. Wang and Y.-H. Chen, Generating large complete momentum gaps in temporally modulated dispersive media, Appl. Phys. Lett. **126**, 221701 (2025).
[40] A. Dikopoltsev, Y. Sharabi, M. Lyubarov, Y. Lumer, S. Tsesses, E. Lustig, I. Kaminer, and M. Segev, Light

emission by free electrons in photonic time-crystals, Proc. Natl. Acad. Sci. U.S.A. **119**, e2119705119 (2022).
[41] H. Li, S. Yin, H. He, J. Xu, A. Alù, and B. Shapiro, Stationary charge radiation in anisotropic photonic time crystals, Phys. Rev. Lett. **130**, 093803 (2023).
[42] M. Lyubarov, Y. Lumer, A. Dikopoltsev, E. Lustig, Y. Sharabi, and M. Segev, Amplified emission and lasing in photonic time crystals, Science **377**, 425 (2022).
[43] M. Lyubarov, A. Dikopoltsev, O. Segal, Y. Plotnik, and M. Segev, Controlling spontaneous emission through the preparation of a photonic time-crystal, Opt. Express **32**, 39734 (2024).
[44] J. Park, K. Lee, R.-Y. Zhang, H.-C. Park, J.-W. Ryu, G. Y. Cho, M. Y. Lee, Z. Zhang, N. Park, W. Jeon, J. Shin, C. T. Chan, and B. Min, Spontaneous emission decay and excitation in photonic time crystals, Phys. Rev. Lett. **135**, 133801 (2025).
[45] K. Lee, M. Kyung, Y. Kim, J. Park, H. Lee, J. Choi, C. T. Chan, J. Shin, K. W. Kim, and B. Min, Spontaneous emission and lasing in photonic time crystals, arXiv:2507.19916.
[46] N. Wang, Z.-Q. Zhang, and C. T. Chan, Photonic Floquet media with a complex time-periodic permittivity, Phys. Rev. B **98**, 085142 (2018).
[47] H. Kazemi, M. Y. Nada, T. Mealy, A. F. Abdelshafy, and F. Capolino, Exceptional points of degeneracy induced by linear time-periodic variation, Phys. Rev. Appl. **11**, 014007 (2019).
[48] N. Wang, B. Hong, and G. P. Wang, Higher-order exceptional points and enhanced polarization sensitivity in anisotropic photonic time-floquet crystals, Opt. Express **32**, 40092 (2024).
[49] A. Pick, B. Zhen, O. D. Miller, C. W. Hsu, F. Hernandez, A. W. Rodriguez, M. Soljačić, and S. G. Johnson, General theory of spontaneous emission near exceptional points, Opt. Express **25**, 12325 (2017).
[50] K. Pang, M. Z. Alam, Y. Zhou, C. Liu, O. Reshef, K. Manukyan, M. Voegtle, A. Pennathur, C. Tseng, X. Su *et al.*, Adiabatic frequency conversion using a time-varying epsilon-near-zero metasurface, Nano Lett. **21**, 5907 (2021).
[51] T. Guo *et al.*, Plasmonic metamaterial time crystal, arXiv:2510.02845.
[52] A. Cartella, T. F. Nova, M. Fechner, R. Merlin, and A. Cavalleri, Parametric amplification of optical phonons, Proc. Natl. Acad. Sci. U.S.A. **115**, 12148 (2018).
[53] J. Sloan, N. Rivera, J. D. Joannopoulos, and M. Soljačić, Casimir light in dispersive nanophotonics, Phys. Rev. Lett. **127**, 053603 (2021).
[54] J. Park, H. Cho, S. Lee, K. Lee, K. Lee, H. C. Park, J.-W. Ryu, N. Park, S. Jeon, and B. Min, Revealing non-Hermitian band structure of photonic Floquet media, Sci. Adv. **8**, eabo6220 (2022).
[55] A. Raman and S. Fan, Photonic band structure of dispersive metamaterials formulated as a Hermitian eigenvalue problem, Phys. Rev. Lett. **104**, 087401 (2010).
[56] See Supplemental Material at http://link.aps.org/supplemental/10.1103/gttv-6lqc for details on our formalism and complementary results, which includes Refs. [57–60].
[57] S. M. Barnett, B. Huttner, and R. Loudon, Spontaneous emission in absorbing dielectric media, Phys. Rev. Lett. **68**, 3698 (1992).
[58] S. A. R. Horsley and T. G. Philbin, Canonical quantization of electromagnetism in spatially dispersive media, New J. Phys. **16**, 013030 (2014).
[59] F. Thouin, D. M. Myers, A. Patri, B. Baloukas, L. Martinu, A. I. Fernández-Domínguez, and S. Kéna-Cohen, Field enhancement and nonlocal effects in epsilon-near-zero photonic gap antennas, ACS Nano **19**, 7996 (2025).
[60] Y. Sun, S. Fan, and G. Hu, Formulation of dispersive and dissipative time-varying media as a Floquet matrix eigenproblem, Phys. Rev. Lett. **135**, 156903 (2025).
[61] S. Zhang, J. Dong, H. Li, J. Xu, and B. Shapiro, Longitudinal optical phonons in photonic time crystals containing a stationary charge, Phys. Rev. B **110**, L100306 (2024).
[62] J. Feinberg, D. E. Fernandes, B. Shapiro, and M. G. Silveirinha, Plasmonic time crystals, Phys. Rev. Lett. **134**, 183801 (2025).
[63] N. Chamanara, Z.-L. Deck-Léger, C. Caloz, and D. Kalluri, Unusual electromagnetic modes in space-time-modulated dispersion-engineered media, Phys. Rev. A **97**, 063829 (2018).
[64] E. Galiffi, P. A. Huidobro, and J. Pendry, An Archimedes' screw for light, Nat. Commun. **13**, 2523 (2022).
[65] J. Dong, S. Zhang, H. He, H. Li, and J. Xu, Nonuniform wave momentum band gap in biaxial anisotropic photonic time crystals, Phys. Rev. Lett. **134**, 063801 (2025).
[66] J. Wiersig, Petermann factors and phase rigidities near exceptional points, Phys. Rev. Res. **5**, 033042 (2023).
[67] J. Ren, S. Franke, B. Van Drunen, and S. Hughes, Classical Purcell factors and spontaneous emission decay rates in a linear gain medium, Phys. Rev. A **109**, 013513 (2024).
[68] While these poles lead to an ill-defined dissipated power, we only approach them in all of our computations to keep convergent results.
[69] J. E. Sustaeta-Osuna, T. F. Allard, F. J. García-Vidal, and P. A. Huidobro, Near-field gain and far-field control via a plasmonic time crystal slab, arXiv:2509.16153.
[70] P. W. Milonni, Why spontaneous emission?, Am. J. Phys. **52**, 340 (1984).
[71] J. T. Mendonça, A. Guerreiro, and A. M. Martins, Quantum theory of time refraction, Phys. Rev. A **62**, 033805 (2000).
[72] A. Ganfornina-Andrades, J. E. Vázquez-Lozano, and I. Liberal, Quantum vacuum amplification in time-varying media with arbitrary temporal profiles, Phys. Rev. Res. **6**, 043320 (2024).
[73] M. S. Mirmoosa, T. Setälä, and A. Norrman, Quantum state engineering and photon statistics at electromagnetic time interfaces, Phys. Rev. Res. **7**, 013120 (2025).
[74] J. E. Sustaeta-Osuna, F. J. García-Vidal, and P. A. Huidobro, Quantum theory of photon pair creation in photonic time crystals, ACS Photonics **12**, 1873 (2025).
[75] J. Bae, K. Lee, B. Min, and K. W. Kim, Quantum electrodynamics of photonic time crystals, Nat. Commun. **17**, 858 (2025).
[76] T. F. Allard, J. E. Sustaeta-Osuna, F. J. García-Vidal, and P. A. Huidobro, Dataset for "Broadband Dipole Absorption in Dispersive Photonic Time Crystals," 2026, 10.5281/zenodo.18483040.